Quantitative Trait Loci Controlling Light and Hormone Response in Two Accessions of *Arabidopsis thaliana*

Justin O. Borevitz,[*,†,1] **Julin N. Maloof,**[*,1] **Jason Lutes,**[*,‡] **Tsegaye Dabi,*** **Joanna L. Redfern,***
Gabriel T. Trainer,[*,‡] **Jonathan D. Werner,**[*,†] **Tadao Asami,**[§] **Charles C. Berry,****
Detlef Weigel[*,††] **and Joanne Chory**[*,‡,2]

*Plant Biology Laboratory, The Salk Institute for Biological Studies, La Jolla, California 92037, †Department of Biology, University of California, La Jolla, California 92037, ‡Howard Hughes Medical Institute, The Salk Institute for Biological Studies, La Jolla, California 92037, §The Institute of Physical and Chemical Research (RIKEN), Wako-shi, Saitama 351-0198, Japan, **Department of Family/Preventive Medicine, University of California, La Jolla, California 92093 and ††Department of Molecular Biology, Max Planck Institute for Developmental Biology, 72076 Tübingen, Germany*

ABSTRACT

We have mapped quantitative trait loci (QTL) responsible for natural variation in light and hormone response between the Cape Verde Islands (Cvi) and Landsberg *erecta* (L*er*) accessions of *Arabidopsis thaliana* using recombinant inbred lines (RILs). Hypocotyl length was measured in four light environments: white, blue, red, and far-red light and in the dark. In addition, white light plus gibberellin (GA) and dark plus the brassinosteroid biosynthesis inhibitor brassinazole (BRZ) were used to detect hormone effects. Twelve QTL were identified that map to loci not previously known to affect light response, as well as loci where candidate genes have been identified from known mutations. Some QTL act in all environments while others show genotype-by-environment interaction. A global threshold was established to identify a significant epistatic interaction between two loci that have few main effects of their own. *LIGHT1*, a major QTL, has been confirmed in a near isogenic line (NIL) and maps to a new locus with effects in all light environments. The *erecta* mutation can explain the effect of the *HYP2* QTL in the blue, BRZ, and dark environments, but not in far-red. *LIGHT2*, also confirmed in an NIL, has effects in white and red light and shows interaction with GA. The phenotype and map position of *LIGHT2* suggest the photoreceptor *PHYB* as a candidate gene. Natural variation in light and hormone response thus defines both new genes and known genes that control light response in wild accessions.

P LANT development is coordinated to optimize the amount of light available for photosynthesis. There is an elaborate control of plant responses to light, with a variety of photoreceptors at the top of different light response signaling hierarchies (Neff *et al.* 2000). The red/far-red light-absorbing phytochromes and the blue/UV-A absorbing cryptochromes perceive light quality and quantity and direct the plant to modify its developmental program. Cotyledon opening and inhibition of hypocotyl length (which are part of the de-etiolation response), shade avoidance, and flowering time are just some of the developmental phenotypes controlled by light. In nature, latitude, climate, vegetation, and terrain create different light environments, requiring plants to modify their light responses. For example, when plants sense light rich in far-red, indicative of shade and/or competition, many plants respond by stem and petiole elongation and accelerated flowering. The hypocotyl length of young seedlings is also affected by light quality and quantity. The adaptive nature of plant light responses is of great interest (Casal and Smith 1989; Smith 1995; Schmitt *et al.* 1999; Maloof *et al.* 2000). Wide genetic variation exists in hypocotyl length in response to light among Arabidopsis accessions (Maloof *et al.* 2001). This variation can be exploited using quantitative trait loci (QTL) mapping to discover new genes and new alleles of known genes in light signaling.

Traditional genetics and other molecular approaches in Arabidopsis have provided a signal transduction framework (Neff *et al.* 2000) upon which new genes discovered from natural populations can be integrated. Arabidopsis plants with mutations in the *PHYTOCHROME B* gene have reduced light sensitivity and elongate much more than wild type under equal light intensities (Reed *et al.* 1993). Responses to light, such as hypocotyl elongation, are also affected by hormones of the gibberellin (GA) and brassinosteroid (BR) classes (Chory and Li 1997). GAs promote cell elongation in the hypocotyl, a response that is attenuated by *PHYB* (Reed *et al.* 1996). In the dark, photomorphogenic growth is suppressed, and this suppression requires BRs. Consequently, Arabidopsis and rice mutants that fail to make or perceive BRs incorrectly de-etiolate in the dark (Li *et al.* 1996; Li

and Chory 1997; Yamamuro *et al.* 2000). Application of the brassinosteroid biosynthetic inhibitor brassinazole (BRZ) mimics BR deficiency, also causing wild-type plants to de-etiolate in the dark (Asami and Yoshida 1999; Asami *et al.* 2000). Apart from seedling development, GAs and BRs affect many other developmental processes that are also controlled by light. The photoreceptor signaling pathways overlap and interact with the hormone signaling pathways, enabling plants to modify their development in response to changing environmental signals.

Understanding the cross talk between these signaling pathways has been challenging since it requires careful observation in many specific light and hormone conditions. Dissecting light signals away from internal hormone control is difficult using traditional genetics. Mutants identified in screens for seedlings altered in hypocotyl length, a common measure of light sensitivity, often show pleiotropic phenotypes due to defects in hormone production or response (Li and Chory 1997; Neff *et al.* 1999; Tian and Reed 1999; Hsieh *et al.* 2000; Zhao *et al.* 2001). To determine which light and hormone response pathways naturally, polymorphic loci affect quantitative mapping can be done in multiple environments. QTL that map to similar locations in different environments may affect multiple photoreceptor pathways or may represent variation in linked genes. Tests of genotype-by-environment interaction ($G \times E$) can confirm unique environment effects when QTL are only detected in a subset of environments. Thus, mapping QTL in different environments can dissect responses to light and hormonal control of hypocotyl length.

There are several advantages to using natural populations to discover genes affecting light response (Alonso-Blanco and Koornneef 2000). Traditional genetic screens for loss-of-function mutations affecting light responses fail to identify both redundant and essential genes and in addition are limited to the genetic complement of commonly used laboratory strains. Subtle phenotypes will also likely be missed without a rigorous quantitative measurement. QTL mapping has the advantage of simultaneous detection of multiple genes that may have small effects, as well as detection of interactions between genes (epistasis) and interactions between genes and environments. In addition, change-of-function mutations and viable polymorphisms in essential genes may occur in wild populations. Perhaps most interestingly, the genes identified from natural populations may have ecological relevance and provide clues about the molecular nature of evolution. The natural variation in wild Arabidopsis accessions is extensive and represents a largely untapped pool of genetic polymorphisms (Alonso-Blanco and Koornneef 2000). Tools such as a complete genome reference sequence, saturating knockout collections, large numbers of polymorphic markers, and ease of transformation make Arabidopsis an excellent model to further characterize alleles that

underlie natural quantitative variation (Krysan *et al.* 1999; Parinov *et al.* 1999; Arabidopsis Genome Initiative 2000). Recombinant inbred lines (RILs) are available and allow a detailed investigation of variation between two parental strains. A disadvantage, however, is that QTL identify large chromosome intervals that may represent multiple genes with small effect.

Methods for detecting QTL depend on the size and type of population analyzed, the number of markers, and the statistical method. RILs allow the inherent environmental error to be reduced by replication, providing a powerful system of QTL analysis. Currently, the statistical methods of composite interval mapping (CIM; Zeng 1994) or multiple QTL model mapping (MQM; Jansen and Stam 1994) have the advantage of allowing background markers to explain variation due to QTL outside the scan region, thereby increasing precision and power to detect QTL within the scan region.

The Arabidopsis RIL population derived from a cross between the Cape Verde Islands accession and the Landsberg *erecta* laboratory strain has been an important tool for the analysis of complex traits (Alonso-Blanco *et al.* 1998b). This population has been used to map QTL responsible for flowering time, seed size and other life history traits, circadian rhythm, and sugar composition and seed storability (Alonso-Blanco *et al.* 1998a, 1999; Bentsink *et al.* 2000; Swarup *et al.* 1999). A different RIL population was used in an elegant study of natural variation in light signaling that revealed genetic differences in the very low fluence response (VLFR) between the Landsberg *erecta* (L*er*) and Columbia (Col) accessions (Yanovsky *et al.* 1997). Two *VLF* QTL were identified that control cotyledon opening under short pulses of far-red light.

Here we used the L*er*/Cvi RIL set to map QTL in seven light and hormone environments. Multiple QTL were identified, some of which act across different light environments, whereas others showed genotype-by-environment interaction. Three QTL were confirmed in near isogenic lines, which define new loci, as well as loci with candidate genes. Moreover, this multienvironment analysis allows QTL to be organized into a genetic framework that can explain natural variation in different photoreceptor pathways.

MATERIALS AND METHODS

Plant material: The RIL set derived from a cross between Cvi and L*er* accessions was used for these studies (Alonso-Blanco *et al.* 1998b). Seeds of 162 RILs and the parents (CS22000), Col-1 (CS3176), and the Col-1 *er-2* (CS3401) mutation were obtained from the Arabidopsis Biological Resource Center (ABRC) in Columbus, Ohio (http://www.arabidopsis.org) and used directly for hypocotyl measurements. Lan-1 (La *ERECTA*) was obtained from Carlos Alonso-Blanco. F_1 hybrids were made by reciprocal crosses for L*er* $\times$ Cvi F_1 (L*er* female) or Cvi $\times$ L*er* F_1 (Cvi female).

Growth conditions: Seeds were sterilized in 1.5-ml microcen-

trifuge tubes for 10 min in 70% ethanol, 0.01% Triton X-100, followed by a 10-min wash with 95% ethanol, and then resuspended in 1 ml sterile water. After imbibition overnight at 4° in the dark, seeds were placed individually onto 0.7% phytagar plates containing ½ Murashige and Skoog salts using a Pipetman. Seedlings were spaced at a uniform density so that they did not shade each other. Plates were kept at 4° in the dark for another 3 days, followed by 4 hr of 120 μE m^{-2} sec^{-1} white light to induce germination. Further incubation was at 23°. Preliminary experiments in six conditions (all except dark) with Cvi, L*er*, and most of the CvL RILs revealed substantial variation in hypocotyl lengths among lines and slight variation from week to week and from plate to plate (data not shown). For the results reported here, all light environments and all RILs were done in the same week to minimize week-to-week and week-to-plate variation. Furthermore the number of RILs per plate was increased to 12, providing better statistical control of plate-to-plate variation. Plates were rotated within each incubation chamber every 12 hr for the duration of the experiment to reduce variation among plates within each incubator. Ideally, the entire experiment would be replicated several times over to reduce the contribution of uncontrolled variation in the observed differences between RILs and light environments and to provide precise estimates of the magnitudes of the components of variation. Without such replication, differences due to uncontrolled variation between growth conditions in different incubators could be attributed to light environments and lead to spurious genotype-by-light environment associations. However, a single run of 162 RILs under seven light environments requires ∼240 person-hours to perform. From the preliminary studies we believed that extraneous variation could be controlled sufficiently to obtain useful results from a single-week experiment alone. In all, 15–30 seedlings of each of 162 CvL RILs, Cvi, L*er*, reciprocal F$_1$ hybrids, and photoreceptor mutants were arrayed in groups of 12 lines per plate across 15 plates. This was replicated for the seven environmental conditions.

Light/hormone conditions: Incubators used for all environments were Percival model E30B (Percival Scientific, Boone, IA). One incubator (Percival E30LED) was equipped with LED lights and used for the far-red environment. Neutral density screens were used to vary light fluence rate. Light measurements were made with a LI-1800 instrument (Li-Cor, Lincoln, Nebraska). We wanted to identify a fluence rate that would maximize the subtle variation in light sensitivity seen in natural populations. Pilot experiments showed that at high light fluence rates CvL RILs had relatively uniform, short hypocotyls and at low light fluence rates CvL lines were much longer but more variable. We chose intermediate light fluence rates, from a fluence response curve, for each light condition, where the broad-sense heritability was maximized for subsequent experiments. White light was provided by three 35-W cool white fluorescent bulbs and two 25-W incandescent bulbs. The photosynthetic active radiation (PAR, 400–700 nm) was 35 μE m^{-2} sec^{-1}, the Pfr/P ratio was 0.72 (KENDRICK and KRONENBERG 1994, p. 268), and the R/FR ratio (655–665 nm)/(725–735 nm) was 1.3. The same light conditions were replicated in another incubator for the GA environment except that 30 μM GA$_3$ (Sigma, St. Louis) was added to the medium. Blue light (PAR = 4 μE m^{-2} sec^{-1}) was provided by three 20-W cool-white fluorescent bulbs and a filter that blocked light above 550 nm. Red light (PAR = 35 μE m^{-2} sec^{-1}) was provided by three 20-W Gro-Lux fluorescent bulbs (Osram Sylvania, Danvers, MA) and a red filter that blocked light below 600 nm. Far-red light (0.5 μE m^{-2} sec^{-1}; 700–730 nm) was provided by LED lights. The same incubator was used for the dark and BRZ environments, and plates were wrapped in aluminum foil and received no further light after the 4-hr

germination light pulse. A dose response curve, using different concentrations of the brassinosteroid biosynthetic inhibitor BRZ 91, identified 0.75 μM as the optimum concentration to maximize the heritability. A total of 0.75 μM BRZ (synthesized at RIKEN) was used unless otherwise indicated.

Hypocotyl length measurements: On day 2, poor germination was scored in white light as 1 or 0. Most lines had already germinated (and were scored as "0"), but 14 lines (CvL nos. 1, 3, 8, 15, 16, 22, 24, 27, 38, 39, 152, 185, 186, and 188) had not (and were scored as "1"). All lines except CvL 3 germinated by day 3 and were measured on day 7. The germination state seen in white light was representative of all conditions and likely reflected both environmental and genetic variation in the state of the seeds rather than light response. Therefore, germination was used as a covariate in subsequent analyses. Seedlings were transferred to acetate sheets containing moist tissue paper and scanned on a flat bed scanner. Hypocotyl lengths were measured in millimeters using National Institutes of Health (NIH) image version 1.62 (http://rsb.info.nih.gov/nih-image). The effect of the covariate germination on hypocotyl length and the average number of seedlings measured in each environment are shown in Table 1.

Statistical analysis: Data analysis was performed using the statistical package R (IHAKA and GENTLEMAN 1996; http://www.R-project.org/). Hypocotyl length data are approximately normally distributed, so no transformation was needed. Hypocotyl length was fit using a statistical model that is described in detail below. Briefly, hypocotyl lengths were fit by a mixed-effects linear model with terms for germination, plate, and RIL. RIL and plate were modeled as random effects with RIL nested under plate; germination status was modeled as a fixed effect. Data for each light environment were fit separately. The variation due to plate, RIL, and residual variation is shown in Table 2. The relative variation explained by line means is an estimate of the broad-sense heritability. Best linear unbiased predictors (BLUPs) of RIL means under this model were used for QTL mapping; those lines showing poor germination had their means augmented by the coefficient for germination state. Note that these BLUPs of RIL means implicitly omit the plate effects, and this reduces the uncontrolled variation in the trait for QTL mapping. Calculations used the linear mixed effects (lme) function in the "nlme" package to R (PINHEIRO and BATES 2000). The genetic correlation between environments (r_{GE}) was calculated using $\text{cov}_{12}/(\sigma_{L1}\sigma_{L2})$, where cov_{12} is the covariance in line means, corrected for germination and plate effect, and σ_{L1} and σ_{L2} are square roots of among-line variances from the linear mixed-effects model (ROBERTSON 1959). Here BLUPs of RIL means used a model with RIL effects as fixed effects; this leads to unbiased estimates of cov_{12} when the reduction in degrees of freedom is accounted for. The coefficient of genetic variation CV_G was calculated for each environment by dividing σ_{L1} by the grand mean of line means and multiplying by 100. Confidence intervals for r_{GE} and CV_G were calculated, using a "leave one out" jackknife procedure on 161 lines (EFRON and TIBSHIRANI 1993).

The model for the dependence of hypocotyl length on germination status, RIL identity, and plate effects was

$$y_{ij} = X_i\beta + Z_i\Gamma_{\text{RIL}} + W_i\Gamma_{\text{plate}} + \varepsilon_{ij}, \qquad (1)$$

where y_{ij} are the measurements of hypocotyl length under a single light environment with $i = 1, \ldots, 161$ indexing the 161 RILs and $j = 1, \ldots, n_i$ indexing the seedlings of the ith RIL. $X_i = (1, \text{germ}_i)$, where germ$_i$ = 1 if germination was poor and 0 otherwise. $\beta = (\beta_0, \beta_1)'$ is a column vector of two unknown coefficients; β_0 is the mean under good germination and β_1 is the increment due to poor germination. Z_i is a row vector of 161 elements all of which are zero except for the ith, which is 1. $\Gamma_{\text{RIL}} \sim N(0, \delta^2_{\text{RIL}}I_{161\times161})$ is a column vector of

161 elements. W_i is a row vector of 14 elements, all of which are zero except for the kth, which is 1 when RIL i was incubated on plate k such that $\Sigma_k(\Sigma_i Z_i' W_i)_k = 1_{161 \times 14}$ (*i.e.*, lines "nest" within plates). $\Gamma_{\text{plate}} \sim N(0, \delta^2_{\text{plate}} I_{14 \times 14})$ is a column vector of 14 elements and $\varepsilon_{ij} \sim N(0, \sigma^2)$ is the residual and independent of other model terms. The phenotypic means are taken as $\tau_i = \beta_0 + Z_i \Gamma_{\text{RIL}}$ and estimates are obtained by replacing the respective parameters with restricted maximum-likelihood (REML) estimates. These estimators are best linear unbiased, so phenotypic means based on τ_i are the BLUPs under this model.

QTL analysis: The CvL RILs had been previously genotyped (ALONSO-BLANCO *et al.* 1998b), using amplified fragment length polymorphisms (AFLP; VOS *et al.* 1995) and cleaved amplified polymorphic sequences (CAPS) markers (KONIEC-ZNY and AUSUBEL 1993). Marker data and the genetic map were obtained from the web at the Nottingham Arabidopsis Stock Center (http://nasc.nott.ac.uk/). We used 163 of the 293 available markers that mapped to unique genetic loci and that had been genotyped on an average of 160 out of 162 RI lines. The BLUP data representing the line mean coefficients corrected for germination and plate effect were used as the phenotypic values for QTL mapping. The CIM (ZENG 1994) function of QTL Cartographer (http://statgen.ncsu.edu/qtlcart/cartographer.html) was used to map QTL. Background markers were chosen using the forward/backward stepwise multiple regression of SR map at a P value of 0.001. When SR map chose adjacent background markers in different environments, QTL models were tested where the same background marker was used in each environment to optimize the LOD score and minimize the LOD support interval. The numbers of background markers ranged from four to seven and are shown in Figure 3. Thresholds in each environment were set internally by running sets of 5000 permutations (DOERGE and CHURCHILL 1996). In each environment, a LOD score of 3.43–3.63 (depending on light environment) corresponded to an experiment-wise P value of 0.01 as determined by permutations. Instead of using seven different thresholds we used the largest one. A LOD of ~2.8 would correspond to $P = 0.05$. We used a window size of 1 cM because hypocotyl length has high heritability, many QTL were in tight linkage, and many lines and many markers were used in this experiment. QTL maps with larger window sizes (1–10 cM) gave broader QTL peaks; however, the two LOD support intervals were equivalent to the 1-cM window size map. Generally the width of QTL peak was defined by the flanking markers, at various window sizes.

Recombinant inbred line-by-environment testing: The RILs are nested within plates in each light environment, so there is no "RIL-by-light environment-by-replicate" term to use as the error term for the "RIL-by-light environment" interaction. To test this interaction, two approaches were used. One was the sequential F-test of the RIL-by-light environment interaction term in a model including terms for line, light environment, plate, germination, and the germination-by-light environment interaction. In the absence of spatial or other effects on plates that increase between-RIL variation on a plate without also increasing "within RIL" variation, this is a powerful and appropriate test. The other test refers Tukey's "1 d.f. for interaction" statistic to its distribution under permutation of RIL interaction terms within plates; this yields a correct P value even in the presence of uncontrolled variation within RIL on a plate, but generally has limited power. For the first approach, Equation 1 and definitions above are extended as

$$y_{ijk} = \tilde{X}_{ik}\tilde{\beta} + Z_i\tilde{\Gamma}_{\text{RIL}} + \tilde{Z}_{ik}\Gamma_{\text{RIL-light}} + \tilde{W}_{ik}\tilde{\Gamma}_{\text{plate}} + \varepsilon_{ijk}, \quad (2)$$

where k indexes the light environment, $\tilde{X}_{ik} = X_i \otimes L_k$, $\tilde{Z}_{ik} = Z_i \otimes L_k$, and $\tilde{W}_{ik} = W_i \otimes L_k$ with L_k being a 1×7 vector with a 1 in the kth element and zeroes elsewhere. $\varepsilon_{ijk} \sim N(0, \sigma^2_k)$ are independent residuals. Other terms on the right-hand

side are suitably sized vectors of coefficients following the normalizations $\Sigma_i(\tilde{\Gamma}_{\text{RIL}})_i = 0$, $\Sigma_i(\tilde{\Gamma}_{\text{RIL-light}})_{7(i-1)+k} = 0$, $\Sigma_k(\tilde{\Gamma}_{\text{RIL-light}})_{7(i-1)+k} = 0$, summing i over 1, . . . , 161 and k over 1, . . . , 7. The mean square for the RIL-by-light environment interaction, $\tilde{Z}_{ik}\tilde{\Gamma}_{\text{RIL-light}}$, has 876 d.f. after accounting for the other terms and the F-statistic takes the residual mean square to be the error. The Tukey 1 d.f. for interaction statistic (SCHEFFÉ 1959, section 4.8) decomposes the sum of the squared RIL-by-light environment terms into two parts,

$$SS_{\text{G}} = \frac{\left(\sum_{i=1}^{7}\sum_{j=1}^{161}\hat{\alpha}_i(\hat{\tilde{\Gamma}}_{\text{RIL}})_j(\hat{\tilde{\Gamma}}_{\text{RIL-light}})_{7(j-1)+i}\right)^2}{\sum_{i=1}^{7}\hat{\alpha}_i^2\sum_{j=1}^{161}(\hat{\tilde{\Gamma}}_{\text{RIL}})_j}$$

$$SS_{\text{res}} = \sum_{i=1}^{7}\sum_{j=1}^{161}(\hat{\tilde{\Gamma}}_{\text{RIL-light}})^2_{7(j-1)+i} - SS_{\text{G}},$$

where

$$\hat{\alpha}_i = \hat{\tilde{\beta}}_{2i-1} - \frac{1}{7}\sum_{i=1}^{7}\hat{\tilde{\beta}}_{2i-1}. \quad (3)$$

The statistic is $F = SS_{\text{G}}/(SS_{\text{res}}/\text{d.f.})$, taking d.f. as 875. A permutation test can be constructed by permuting $(\hat{\tilde{\Gamma}}_{\text{RIL-light}})_{7(j-1)+i}$ with respect to the index j and calculating F under each permutation. Possible plate effects should be preserved in the reference distribution, so permutations of j must respect the assignment of RILs to plates. This type of permutation honors the normalizations above.

Multienvironment QTL mapping: The multitrait CIM (mCIM) program JZmapqtl in QTL Cartographer was used (JIANG and ZENG 1995). mCIM mapping calculates a joint likelihood to detect QTL in multiple environments and a genotype-by-environment likelihood to determine if QTL are specific to certain environments. Light and hormone interactions were tested separately by including four light environments (white, blue, red, and far-red) in one analysis, white light and GA in a second analysis, and dark and BRZ in a third. A common set of background markers was used for each analysis (Figure 3, Table 4), to avoid problems of overparameterization. When SRmap chose adjacent background markers closer than 3 cM apart in different environments, a common marker was chosen that was selected in the majority of environments. An experiment-wise $P = 0.01$ threshold for both the joint likelihood (main effects) and G × E likelihood was determined separately for each analysis by performing 5000 permutations (DOERGE and CHURCHILL 1996; G × E LOD = 5.7 for four light environments and 3.6 for each of the hormone comparisons). These routines were provided by Chris Basten and are available upon request. The likelihood of the G × E test at each QTL was compared to the threshold to determine if that QTL showed a significant G × E interaction. This occurs when the estimated QTL effect is different from the joint effect in at least one of the tested environments.

Tests of epistasis: We tested interactions between QTL and then performed an exhaustive search for pairwise marker interactions using BQTL. Each environment was analyzed separately and included main effect QTL as background markers (Figure 3, Table 4) and the covariate germination. A total of 43,956 pairwise tests were done between 296 loci. These included 163 actual markers and 133 pseudomarkers, at marker intervals <2 cM, creating an ~2-cM walking speed. The test statistic is the LOD score difference between a model with only additive effects and one that included an epistatic term. Thresholds for statistical tests used a sequential permutation procedure (NETTLETON and DOERGE 2000) to ensure that enough permutations were performed to assert that each test attained (or failed at) $P = 0.05$. This is discussed in detail below. A total of 5000 permutations were done in the white light environment. Each permutation tested 43,956 pairs of

markers. A LOD score of ~4.6 corresponded to an experiment-wise threshold of $P = 0.05$ and was similar across light environments. The effect of the epistatic interaction is shown as $4i$ (Table 4), which represents the difference between the homotypic and heterotypic means (JUENGER *et al.* 2000). The interacting loci on chromosome 5 were also detected as the pair with the largest test statistic from the preliminary experiment in white light.

The maximum-likelihood method provides good power for detecting epistasis (KAO 2000) but requires more time for computation than linear methods for QTL mapping (KNAPP *et al.* 1990; HALEY and KNOTT 1992). To obtain correct P values with a model with covariates and additional loci, a permutation procedure is needed—further increasing the computational burden. Hybrid procedures for QTL mapping that are linear with respect to some, but not all, loci (JANSEN 1993; ZENG 1994) are widely used and provide some of the benefits of a full maximum-likelihood approach at a reduced computational cost. Such a hybrid approach and an associated permutation test for scanning for epistasis were implemented as follows. The log-likelihood used for scanning for epistasis is

$$L(\alpha, \beta, \gamma_1, \gamma_2, \gamma_{12}, \theta, \sigma^2; y, x, l_1, l_2)$$

$$= \sum \log \sum_{j=1}^{2} \sum_{k=1}^{2} \phi(y_i; \mu_{ijk}, \sigma^2) \pi_{Z|M}(Z_{l_1 l_2} = (z_j, z_k) \mid M = m_i), \quad (4)$$

where

$$\mu_{ijk} = \alpha + x_i\beta + z_j\gamma_1 + z_k\gamma_2 + z_jz_k\gamma_{12} + E_{Z|M}(z_{l_3}, \ldots, z_{l_n} \mid m_i)\theta, \quad (5)$$

$y_i = \hat{\tau}_i$, α is the intercept, x_i is zero if the ith line had good germination and one otherwise with β as the coefficient for germination, j and k index the parental lines of the alleles at loci l_1 and l_2 being tested for epistasis, $z_j = 2(j - 1.5)$, $z_k = 2(k - 1.5)$, γ_1 and γ_2 are the main effects at those alleles and γ_{12} is the epistatic effect, $E_{Z|M}(z_{l_3}, \ldots, z_{l_n}|m_i)$ is the expectation of a vector of z's corresponding to $n - 2$ other loci given the marker information for subject i and θ is a vector of coefficients, $\pi_{Z|M}(Z = (z_j, z_k)|M = m_i)$ is the probability that the two loci are in states j and k given the marker information for subject i, σ^2 is the residual variance, and $\phi(y; \mu, \sigma^2)$ is the normal density function. The maximum-likelihood solution of (4) and (5) with respect to all of the coefficients is carried out. In addition, the maximum-likelihood solution under $\gamma_{12} = 0$ (no epistasis) is found. The log-likelihood ratio statistic $X^2(l_1, l_2) = 2(\sup_\nu L(\nu; y, x, l_1, l_2) - \sup_{\nu_0} L(\nu_0; y, x, l_1, l_2))$ is formed for all pairwise combinations of loci, $l_1 = 1, \ldots, 295, l_2 = l_1 + 1, \ldots, 296$, taking ν as the vector of free parameters and ν_0 as that vector with γ_{12} fixed at zero. Statistical significance is ascertained via permutation testing using the "residual empirical threshold" method (DOERGE and CHURCHILL 1996). Predicted values and residuals are formed using a model in which $\gamma_1 = \gamma_2 = \gamma_{12} = 0$; *i.e.*, only the germination effect and the effects of the $n - 2$ loci used in all models are included. A new vector of trait values is formed by adding the fitted values to a permutation of the residuals from that model. The log-likelihood ratio statistic is found as above for every combination of loci, and the maximum of these is found for each permutation. Attained P values are found as the fraction of permuted maxima that equals or exceeds $X^2(l_1, l_2)$. This produces genome-wide P values that are nominally correct under the null hypothesis of no epistasis anywhere on the genome. However, the randomness in the procedure is considered objectionable especially when claiming to have attained a fixed significance level. This can be overcome by following the recommendations of NETTLETON and DOERGE (2000), requiring that the 95% confidence interval for P values exclude 0.05 and 0.01. Calculations were performed by the function "bqtl" available in the R package, *BQTL* (http://hacuna. ucsd.edu/bqtl and http://cran.r-project.org).

QTL effect estimation: QTL effects were estimated by applying the method of maximum likelihood to the QTL model (KAO 2000). This model included main effect QTL identified by CIM, significant epistatic loci, and the covariate germination. QTL effects are estimated using a likelihood analogous to (4) and (5). Since the number of loci is manageably small and there are only a few models to be fit, no use of linearized terms $E_{Z|M}$ is needed, and full maximum-likelihood fitting is used. The modifications required are to replace μ_{ijk} by $\mu_{ij_1, \ldots, j_K} = \alpha + x_i\beta + \Sigma_{k=1}^{K} z_{j_k}\gamma_k + \Sigma_{l=1}^{L} z_{j_{r_l}} z_{j_{s_l}} \gamma_{r_l} \gamma_{s_l}$, where $j_1, \ldots, j_K$ index K loci included in the QTL model, L epistatic terms are included with r_l and s_l indexing the main effects upon which they depend. Obvious modifications are made to the summation and to $\pi_{Z|M}$, the joint allele state probabilities, in (4). These calculations were also performed by the function bqtl available in the R package. The additive effect is shown as $2a$, the difference between homozygous classes. The percentage of change caused by a single QTL is the effect in millimeters ($2a$) divided by the average RIL hypocotyl length for that environment (Table 4) multiplied by 100. The percentage of variance explained for each QTL was determined by squaring the coefficient (a) and by dividing the residual variance in a null model without genetic loci (σ_{rN}^2). Total variance explained was determined as $1 - (\sigma_{rG}^2)/(\sigma_{rN}^2)$, where (σ_{rG}^2) is the residual variance in the model with all genetic terms.

Near isogenic lines: The *LIGHT1* near isogenic line (NIL) was derived from line N42 created to map EDI (ALONSO-BLANCO *et al.* 1998a). N42 contains only 35 cM of Cvi from the top of chromosome 1 in a L*er* background determined by selection against other markers throughout the rest of the genome (gift from Carlos Alonso-Blanco and Maarten Koornneef). N42 was crossed to L*er*, and F_2 plants that had the L*er* allele at *EDI* and were heterozygous at marker g2395 were selected. The *LIGHT1* NIL is an F_3 line (F_3-77), derived by selfing, that is heterozygous for the AFLP marker GD143L-Col and the CAPS marker m235 at 22 and 34 cM on chromosome 1, respectively. After hypocotyl lengths in white light were measured, individual seedlings were genotyped at g2395 as a marker for the *LIGHT1* QTL. The *LIGHT2* and *HYP2* NILs were made by crossing the RIL CvL 125 to L*er*. The CvL125 × L*er* F_2 cross segregates Cvi DNA from 34 to 63 cM on chromosome 2 containing the *PHYB* and *ERECTA* loci, as well as from 84 to 107 cM on chromosome 5. For *LIGHT2*, 100 F_2 plants were measured in white light and genotyped at *PHYB* and *GPA1* as markers for the *LIGHT2* QTL. Interval mapping was done between these two markers. For *HYP2*, F_2 plants were measured in the far-red and BRZ environments and genotyped at *BAS1* (NEFF *et al.* 1999). The additive and dominance effects of each marker were assessed using linear regression.

Genotyping: Genotyping was done using CAPS markers. *GPA1*, g2395, and m235 information was from TAIR (http://www.arabidopsis.org). *PHYB* oligonucleotide primers were 5′ CTGCTGACGAGAACACG 3′ and 5′ GAAAGTTGGCTTAAATGG 3′; L*er* has a *Pst*I restriction site absent from Cvi. *BAS1* oligonucleotide primers were 5′ ATATAATAGGCGTTCATCTAATG 3′ and 5′ CTCGGAGTTCGTACATG 3′; Cvi has an *Acc*I restriction site absent in L*er*. The *BAS1* marker is 170 kb from the *ERECTA* gene, on the same bacterial artificial chromosome (BAC) T9J22.

Data and statistical routines are available on our web page (http://naturalvariation.org).

RESULTS

Genetic variation in CvL RILs: Light quality (wavelength) and light quantity (fluence rate) affect hypocotyl

TABLE 1

Summary table of CvL RILs

	White			Blue			Red			Far-red			GA			BRZ			Dark		
	mean	SD	±CI	mean	SD	±CI	mean	SD	±CI	mean	SD	±CI	mean	SD	±CI	mean	SD	±CI	mean	SD	±CI
Cvi-K	7.1	0.5	0.2	9.4	0.6	0.3	11.0	1.0	0.5	5.6	0.6	0.3	10.1	0.7	0.3	10.4	1.5	0.7	17.2	1.5	1.1
Ler-K	4.6	0.5	0.3	5.7	0.4	0.2	6.0	0.6	0.3	4.2	0.4	0.2	6.0	0.5	0.3	6.0	0.6	0.2	15.3	2.1	1.1
Ler × Cvi F$_1$	6.2	1.0	0.7	6.7	1.4	0.7	9.4	1.3	0.6	4.3	0.4	0.2	7.7	1.5	0.9	6.7	1.2	0.9			
Cvi × Ler F$_1$	6.9	1.3	0.8	9.7	0.8	0.7	11.1	0.8	0.6	6.0	0.8	0.7	10.8	0.3	0.3	11.3	1.4	1.2	19.8	2.1	2.1
phyB-5	8.6	0.9	0.6	5.8	0.9	0.5	14.7	1.9	1.5	4.4	0.5	0.2	10.6	1.4	0.8	7.7	0.8	0.3	16.3	0.8	0.5
phyA-201	5.6	0.6	0.3	6.2	0.5	0.4	8.2	1.2	0.6	10.0	1.3	0.5	4.7	0.5	0.3	5.6	0.8	0.3	12.6	0.7	0.5
RIL mean	5.9	1.1	1.3	6.7	1.3	1.5	9.0	1.7	1.9	5.0	0.8	1.0	8.0	1.5	1.7	7.8	1.6	1.8	15.8	1.6	2.0
RIL max	8.4	0.8	0.4	10.0	0.9	0.4	13.9	1.0	0.5	7.6	0.6	0.4	12.2	1.7	0.9	12.5	1.1	0.6	19.1	2.3	1.3
RIL min	3.8	0.4	0.3	4.4	0.5	0.3	6.0	0.8	1.0	3.0	0.3	0.2	4.7	0.4	0.2	5.0	0.6	0.2	12.7	0.9	0.7
Germ (late)	−1.2		0.7	−0.9		0.8	−1.4		1.0	−0.6		0.5	−1.5		0.9	−1.1		0.9	−1.3		1.0
Seedlings per line	14.6	4.7		15.0	3.2		12.8	5.1		20.4	4.8		16.8	4.9		18.7	6.0		11.6	4.2	
Total seedlings	2373			2426			2073			3297			2715			3029			1874		
%CV$_G$	19		2	19		2	19		2	17		2	19		2	20		2	10		1

Mean hypocotyl length, standard deviation, and 95% confidence interval half widths are shown in millimeters for Cvi and Ler parents, F$_1$ reciprocal hybrids, *phyB-5* and *phyA-201* Ler photoreceptor null mutants, the CvL RILs, and the effect of the covariate germination in each of seven environments. The number of seedlings measured per line and in total and the coefficient of variation (CV$_G$ ± 95% confidence interval half widths) are also shown for each environment.
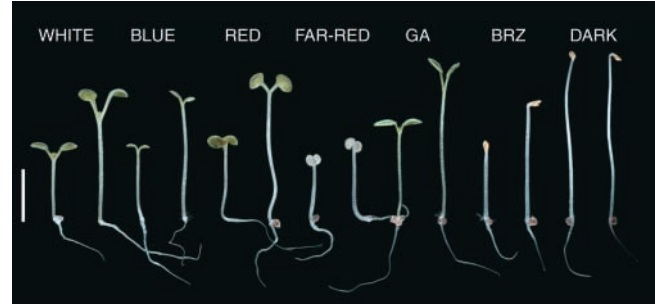

FIGURE 1.—Ler and Cvi seedlings. Pairs of 7-day-old Ler (left) and Cvi (right) seedlings grown in white, blue, red, far-red, GA, BRZ, and dark environments are shown.

length. We chose wavelengths of light that corresponded to the absorption maximum for the red and far-red absorbing forms of phytochrome and blue for cryptochrome to dissect the light responses controlled by individual photoreceptor pathways.

We then measured hypocotyl length of Cvi and Ler parental lines, reciprocal F$_1$ hybrids, 162 Cvi/Ler RILs, and phytochrome mutants in seven different environments. The results are summarized in Table 1. In total, 17,787 hypocotyl length measurements made up the data set. Figure 1 shows the phenotype of the parental lines after 7 days of growth under the different experimental conditions. Cvi was generally less sensitive to light with a longer hypocotyl than the common lab strain Ler (*t*-test $P < 0.05$ all environments). Hypocotyl length differences were dramatic in white, blue, red, GA, and BRZ environments, but less so in the far-red and dark environments. F$_1$ hybrids had long hypocotyls and were generally similar to the Cvi parent (Table 1). The difference between reciprocal crosses is likely due to the maternal effect of the *erecta* mutation (ALONSO-BLANCO *et al.* 1999) as crosses using Ler as females were generally shorter. The distribution of mean hypocotyl lengths among CvL RILs in each environment is broad and continuous, typical of polygenic traits (Figure 2). Transgression was also observed in each environment. The *phyB-5* null mutant has a very severe defect in light signaling in the white and red light environments. Variation of this magnitude was not expected in natural populations. Surprisingly, some transgressive RILs were found to have a hypocotyl length equal to *phyB-5* in white light, and beyond that of *phyB-5* in the GA environment. This may be due to the action of several genes and illustrated the magnitude of natural variation in this trait. In comparison, variation in far-red light was not as dramatic as that caused by a *phyA* null mutant. Nevertheless, the large amount of transgression seen in the far-red environment showed that there was considerable genetic variation segregating, even though the parental lines did not differ by much.

The genetic coefficient of variation (CV$_G$), a unitless measure of genetic variability (HOULE 1992), was ~20%

of the mean for each environment except dark, where it was only 10% of the mean. The variance explained by RILs is an estimate of broad-sense heritability (Table 2). This ranged from 65 to 77% across environments except dark, which was lower (38%) due to a relatively large environmental component. This low level of background variation in the dark environment indicates that the variation seen in other environments was due largely to the specific effects of light and hormone treatments. Tests for RIL-by-environment interactions (see MATERIALS AND METHODS) were highly significant (Table 2).

Response is correlated across environments: We estimated the cross-environment genetic correlation (r_{GE}) between environments and found significant correlations between responses in all light and hormone conditions (Table 3). This indicates that much of the genetic control is shared among environments but that it is not identical. The highest correlation was between white and GA, $r_{GE} = 0.91$. In contrast, the correlation between dark and BRZ is 0.69. Differences in genetic correlations between the hormone environments may be due to true differences in the hormone response. Alternatively, differences in genetic correlations between these environments may reflect differences caused by adding additional GA hormone in one environment and using an inhibitor to remove BR hormone in another. Furthermore differences may reflect variation in endogenous levels of GA and BR levels.

Quantitative trait loci: We first mapped QTL for each environment independently, using different background markers for each trait. The LOD score map is shown for each chromosome in Figure 3. QTL with LOD scores >3.6 ($P < 0.01$ threshold set by permutations) were considered significant. We chose a higher threshold because the many more QTL detected at $P < 0.05$ had rather small effects. A summary of the significant QTL including their effects is shown in Table 4. The effects were estimated by including significant markers and germination as covariates, using a maximum-likelihood approach that included main and epistatic terms (BQTL, see MATERIALS AND METHODS).

We named the QTL according to the environment in which they were detected and the chromosome to which they mapped (Figure 3). Three QTL mapped to chromosome 1. *DARK1* maps to the top (0–7 cM) and was detected only in the dark environment. *LIGHT1* was detected in all light environments and is one of the major QTL, explaining 22% of the phenotypic variance (σ_p) in white light. *LIGHT1* had the highest LOD score of all the QTL in the white, blue, and red environments. The effect of *LIGHT1* was similar in white, blue, and red environments but was weaker in the far-red environment (Table 4). *HYPOCOTYL1* (*HYP1*) contributes to r_{GE} since it was detected in all environments; however, the LOD score was below the threshold in the dark environment (Figure 3). The L*er* allele of the *HYP1* QTL increased hypocotyl length and may explain the
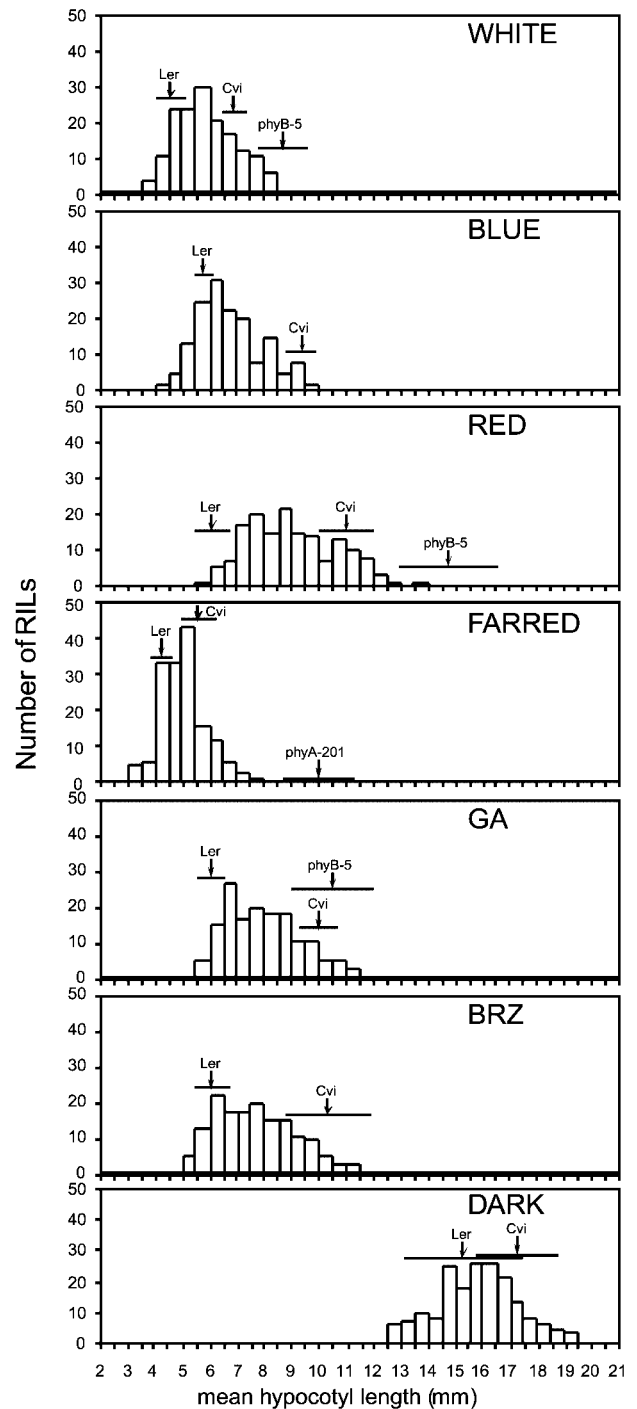

FIGURE 2.—Distribution of CvL RILs. Histograms show the distributions of mean hypocotyl lengths in different light and hormone environments. The mean and standard deviations of L*er*, Cvi, and phytochrome mutants are shown by arrows and lines, respectively.

transgression seen in many environments. *LIGHT2*, a major QTL on chromosome 2 (32–40 cM), was detected in white, red, and GA environments. The largest effect of *LIGHT2* was seen in the GA environment where homozygous allele substitutions caused 1.3 mm change in length and explained 22% of the phenotypic variance.

TABLE 2

Variance components for hypocotyl lengths

	Plate		Line		Error:
	% var	P value	% var	P value	% var
White	2	0.53	75	0	23
Blue	8	0.02	65	0	27
Red	0	1.00	72	0	28
Far-red	0	1.00	68	0	32
GA	3	0.33	77	0	20
BRZ	0	1.00	77	0	23
Dark	4	0.04	38	0	58

	d.f.	F statistic	P value
+RIL × environment	876/16482	15.8	<0.0001
*RIL × environment	1/875	16.4	<0.0001

Each environment had 14 plates and ∼12 RILs per plate. The percentage of variance (% var) explained by lines is an estimate of the broad-sense heritability. + denotes a sequential *F*-test. *Tukey 1 d.f. test is compared to a permutation distribution (see MATERIALS AND METHODS for details).

Another QTL on chromosome 2, *HYPOCOTYL2* (*HYP2*), mapped to the *ERECTA* locus and was detected in the blue, far-red, BRZ, and dark environments. A third QTL, *FARRED2*, was detected only in the far-red environment. On chromosome 3 we detected only one QTL, *RED3*, where again the L*er* allele increases hypocotyl length. Chromosome 4 contained four significant QTL that were specific to single environments, *BRZ4*, *WHITE4*, *BLUE4*, and *FARRED4*. Last, chromosome 5 contained one QTL that was specific to the blue environment, *BLUE5* (0–3 cM). Taken together, multiple QTL were detected across the seven environments that explain up to 61% of the variation in light response (Table 4). A surprisingly large amount of linkage was seen between

QTL (Figure 3). The high genetic correlations among environments can be explained in part by QTL detected in multiple environments as well as linked QTL whose effects are specific to certain environments.

Genotype-by-environment interaction: To understand how the natural variation seen at these light response QTL is controlled across different environments we used mCIM (JIANG and ZENG 1995). A genome scan, using common background markers, was performed in a single joint analysis using white, blue, red, and far-red environments as four traits. All QTL detected using single-environment CIM mapping were confirmed, using mCIM mapping (joint likelihood exceeded the threshold), with the exception of light QTL on chromosome 4 (*BLUE4*, *WHITE4*, and *FARRED4*). Loci where the G × E likelihood exceeded the significance threshold (*P* = 0.01 by permutations) are shown in italics in Table 4. As expected, the QTL unique to single environments or to a subset of environments, *DARK1*, *FARRED2*, *RED3*, *BLUE5*, *LIGHT2*, and *HYP2*, showed significant G × E. *LIGHT1* also showed significant G × E, even though it was detected by single-trait analysis in all light environments, reflecting the fact that *LIGHT1* has a larger effect in white, blue, and red than in the far-red environment. As expected, the *HYP1* QTL did not show G × E.

To assess the effects of the hormone GA, a multitrait analysis was conducted, including the white and GA environments. The only QTL that showed significant G × E was *LIGHT2*, due to the difference in effects at this locus between the GA and white environments. In the GA environment Cvi alleles increased the phenotype by 1.3 mm, whereas in white light, they caused only a 0.7 mm increase (Table 4). However, the effect of *LIGHT2*, expressed as percentage of change in length, is similar between the GA and white environments. The effect of the BR inhibitor BRZ was investigated in the same way

TABLE 3

Genetic correlations among environments

	White	Blue	Red	Far-red	GA	BRZ	Dark
White		0.75 (0.67–0.84)	0.81 (0.73–0.89)	0.53 (0.4–0.66)	0.91 (0.87–0.95)	0.51 (0.36–0.66)	0.59 (0.45–0.74)
Blue			0.78 (0.69–0.88)	0.77 (0.68–0.87)	0.76 (0.68–0.84)	0.65 (0.54–0.76)	0.74 (0.64–0.84)
Red				0.74 (0.63–0.84)	0.83 (0.76–0.91)	0.61 (0.48–0.74)	0.57 (0.43–0.71)
Far-red					0.58 (0.47–0.7)	0.72 (0.6–0.84)	0.66 (0.53–0.79)
GA						0.60 (0.48–0.73)	0.67 (0.53–0.8)
BRZ							0.69 (0.58–0.81)
Dark							

The genetic correlations $cov_{12}/(\sigma_{L1}\sigma_{L2})$ between the environments are shown. The 95% confidence interval of the genetic correlation is below each genetic correlation coefficient.
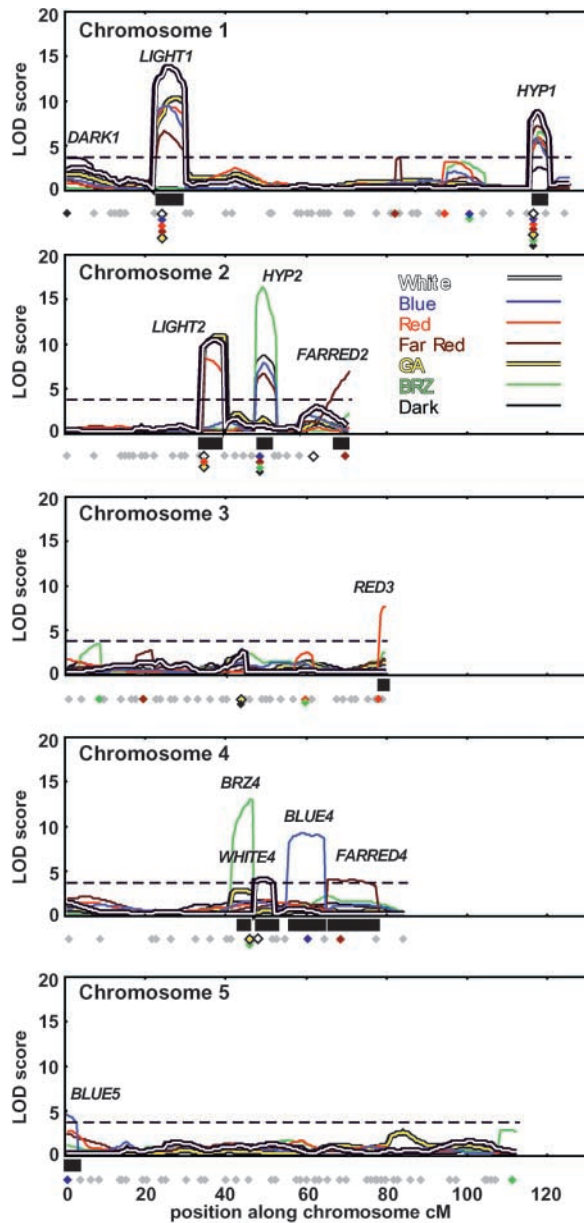
FIGURE 3.—QTL map for light and hormone response. A QTL map generated by composite interval mapping shows the likelihood of odds (LOD) score on the *y*-axis along each chromosome on the *x*-axis. Each color represents a different environment. Markers are shown by diamonds along each chromosome. Background markers are shown as colored diamonds, with colors corresponding to the environment where they were included in the model. The dashed line is LOD 3.6, which represents a $P = 0.01$ threshold set by permutations. 2-LOD support intervals are shown as black bars below the *x*-axis.

using mCIM by including dark and BRZ environments as traits. As expected the unique loci *DARK1* and *BRZ4* showed significant G × E as they were only detected in a single environment. *HYP2* did not show G × E as it has a similar additive effect in dark and BRZ environments, 1.3 and 1.5 mm respectively. However, the difference in effects expressed as percentage of change in

length is dramatic, 8% in dark and 20% in the BRZ environment (Table 4).

Epistatic interactions: We performed a genome scan for pairwise interactions. Each environment was analyzed separately using models that included specific background markers (see MATERIALS AND METHODS). Again an appropriate significance threshold was set by permutations to account for the type of population, any segregation distortion, and the large number of tests. A single epistatic pair was identified in the white light environment that was significant under this stringent criterion (-1.4 mm in white light, Table 4). In all other environments, this pair had an effect (-0.8–1.5 mm) similar to that seen in white light and was point-wise significant ($P < 0.007$). These epistatic loci are linked on chromosome 5, separated by $\sim$15 cM. Forty-four of 162 RILs fall into this recombinant class. The negative interaction coefficient indicates that L*er* and Cvi allele classes act cooperatively in this case. Figure 4 depicts a genetic model that illustrates the statistical epistatic interaction. Apparently, one of these markers acts as a "controller locus." There is an allele-specific interaction that is the basis for the significant epistatic term in the statistical model. When BF.269C is L*er*, allele changes at GH.117C have no effect, but when BF.269C is Cvi, allele changes at GH.117C have a large effect. Thus, BF.269C could act as a controller locus and GH.117C as the "effector locus." By reversing the order of the middle genotypes in Figure 4, GH.117C could be the controller locus governing the direction of the effect of BF.269C. These two genetic models (Figure 4) are equally plausible interpretations of the statistical interaction.

Near isogenic lines: To confirm and better characterize the major QTL, we introgressed them into an isogenic L*er* background. NIL-QTL effects were measured in segregating progeny of a single line to minimize seed variation between different mother plants (Figure 5). The *LIGHT1* NIL is heterozygous and segregates the *LIGHT1* QTL. The effect of *LIGHT1* in an isogenic background confirms the prediction by QTL analysis in the RIL population and also shows that the gene is unlikely to act dominantly ($d/a = -0.4$, $P = 0.52$). The effects of *LIGHT2* and *HYP2* QTL were investigated in an isogenic L*er* background (see MATERIALS AND METHODS). Surprisingly, the less sensitive Cvi allele of *LIGHT2* was dominant ($d/a = 0.8$, $P = 0.002$). The effect of the *HYP2* QTL was confirmed in two environments using CvL125 × L*er* F_2 seedlings. In the far-red environment *HYP2* showed no evidence of a dominant effect ($d/a = -0.1$, $P = 0.82$), whereas in the BRZ environment the Cvi allele of *HYP2* was clearly dominant ($d/a = 1.1$, $P = 6 \times 10^{-5}$).

***ERECTA* and *HYP2*:** The *erecta* mutation segregating in these lines has been shown to have many pleiotropic effects in L*er* (TORII *et al.* 1996). Since the *HYP2* QTL spans the *ERECTA* locus, we wanted to test whether it

TABLE 4

QTL effects in different environments

QTL	Marker	Chrom	2 LOD (cM)	White LOD	White mm	White %l	White %var	Blue LOD	Blue mm	Blue %l	Blue %var	Red LOD	Red mm	Red %l	Red %var	Far-red LOD	Far-red mm	Far-red %l	Far-red %var
									Main effect loci										
1 DARK1	PVV4	1	(0–7)	*14.0*	*1.0*	*21*	*22*	*9.5*	*0.9*	*16*	*16*	*9.4*	*1.3*	*17*	*17*	6.7	0.5	11	10
2 LIGHT1	CD.157C-Col/158L	1	(22–30)	8.8	-0.7	-15	10	5.7	-0.6	-11	8	5.9	-0.6	-8	3	7.2	-0.3	-7	4
3 HYP1	FD.90L-Col	1	(116–121)	*10.6*	*0.7*	*15*	*11*					*8.4*	*1.4*	*18*	*18*				
4 LIGHT2	BF.221L	2	(32–40)																
+5 HYP2	Erecta	2	(47–53)					7.9	0.9	15	14					*6.6*	*0.6*	*13*	*13*
+6 FARRED2	DF.140C	2	(68–71)													6.7	0.2	5	1
7 RED3	GB.97L-Col/99C	3	(76–80)									7.6	-1.0	-13	9				
8 BRZ4	SC5	4	(43–48)																
9 WHITE4	DF.108L-Col	4	(46–52)	4.0	0.4	9	4												
10 BLUE4	FD.167L-Col	4	(55–65)					9.3	0.9	15	13								
11 FARRED4	GH.433L-Col	4	(65–78)													4.0	0.4	10	7
12 BLUE5	FD.207L	5	(0–3)					4.2	0.6	10	6								
									Epistatic loci										
Additive w.EPI1	BF.269C	5	(19–25)		0.0	0													
Additive w.EPI2	GH.117C	5	(36–41)		-0.4	-8													
Interaction	(BF.269C × GH.117C)	5 × 5		5.3	-1.4	-15	10		-0.7	-13			-1.0	-14			-0.6	-13	
Germ					-0.3	-6													
Total variance explained							61				51				45				41

QTL	Marker	Chrom	*2 LOD (cM)	White LOD	White mm	White %l	White %var	GA LOD	GA mm	GA %l	GA %var	Dark LOD	Dark mm	Dark %l	Dark %var	BRZ LOD	BRZ mm	BRZ %l	BRZ %var
									Main effect loci										
1 DARK1	PVV4	1	(0–7)	14.0	1.0	21	22	10.4	1.2	18	17	*3.7*	*0.7*	*5*	*6*				
2 LIGHT1	CD.157C-Col/158L	1	(22–30)	8.8	-0.7	-15	10	5.6	-0.8	-12	7								
3 HYP1	FD.90L-Col	1	(116–121)	10.6	0.7	15	11	*10.9*	*1.3*	*21*	*22*					6.6	-0.8	-12	7
4 LIGHT2	BF.221L	2	(32–40)																
+5 HYP2	Erecta	2	(47–53)									8.6	1.3	9	20	16.6	1.5	23	25
+6 FARRED2	DF.140C	2	(68–71)																
7 RED3	GB.97L-Col/99C	3	(76–80)													*13.2*	*1.3*	*20*	*19*
8 BRZ4	SC5	4	(43–48)																
9 WHITE4	DF.108L-Col	4	(46–52)	4.0	0.4	9	4												
10 BLUE4	FD.167L-Col	4	(55–65)																
11 FARRED4	GH.433L-Col	4	(65–78)																
12 BLUE5	FD.207L	5	(0–3)																
									Epistatic loci										
Additive w.EPI1	BF.269C	5	(19–25)		0.0	0													
Additive w.EPI2	GH.117C	5	(36–41)		-0.4	-8													
Interaction	(BF.269C × GH.117C)	5 × 5		5.3	-1.4	-15	10		-0.5	-8			-0.5	-4			-0.4	-6	
Germ					-0.3	-6													
Total variance explained							61				43				27				48

For each QTL the maximum LOD score, additive effect $2a$ (mm), the percentage of change in length (% l), and the percentage of variance (% var) are shown. Positive effects indicate that the Cvi allele increases the phenotype. Italic type indicates a significant G × E interaction. The additive effects of the markers in the epistatic interaction are also shown. For the epistatic interaction the LOD increase due to the epistatic term, effect $4i$ (mm), percentage of change in length, and percentage of variance explained are shown. + denotes the variance explained is corrected for linkage (Kao 2000). * is the largest 2-LOD interval when the QTL was detected in multiple environments.
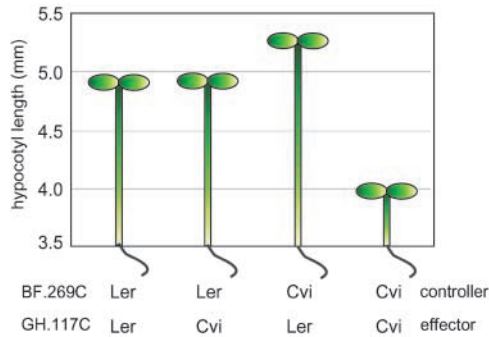
FIGURE 4.—Epistatic interaction. A genetic model is shown of the significant epistatic interaction between two loci on chromosome 5, in the white light environment. BF.269C is shown as a controller locus and GH.117C is shown as the effector locus. Other genetic models are possible.

might correspond to the *erecta* mutation. In the BRZ environment the L*er* allele of *HYP2* acts recessively as does the loss-of-function *erecta* mutation (Figure 5). In contrast, the *HYP2* QTL seems to act additively in the far-red environment. *HYP2* also has an effect in the blue environment (Figure 3, Table 4). We used two alleles of the *erecta* mutation in different backgrounds to determine its effect on hypocotyl length. The Lan-1 (La *ERECTA*) line is isogenic to L*er* (La *erecta*) except that it does not contain the *erecta* mutation (ALONSO-BLANCO and KOORNNEEF 2000). The *er-2* mutation was isolated in the Columbia background. We measured the four genotypes Col *erecta*, La *erecta*, Col *ERECTA*, La *ERECTA* on different concentrations of BRZ and in blue and far-red light (Figure 6). In both Col and La genetic backgrounds *erecta* causes a shortening of hypocotyl length in the dark and at different concentrations of BRZ. This shortening seemed independent of BRZ concentration as *erecta* mutant lines were 0.8 mm shorter at all inhibitor concentrations (Figure 6A), consistent with the *HYP2* QTL not showing a G × E interaction

with BRZ (Table 4). Scale remains a complicating issue; in terms of percentage of change *erecta* has a much larger effect at higher inhibitor concentrations. In blue light *erecta* also has an effect; loss-of-function mutations are 1.0 mm ($P = 0.002$) shorter in both genetic backgrounds (Figure 6B). In far-red light, however, we did not detect a significant effect of *erecta* ($P = 0.56$). Additionally, the *erecta* effect in blue was significantly different ($P < 0.01$) from that in far-red (Figure 6B). We conclude that the effect of *HYP2* in the blue, BRZ, and dark environments is caused by the *erecta* mutation, and another tightly linked gene must be responsible for the effect of *HYP2* in far-red light.

PHYTOCHROME B is a candidate for *LIGHT2*: Arabidopsis *phyB* mutants have elongated hypocotyls in the white and red environments but not in the blue or far-red environments (Table 1). *phyB* mutants are also hypersensitive to GA (REED *et al.* 1996). The phenotype of the *LIGHT2* QTL matches that of *phyB* (Table 4) and *LIGHT2* maps very close to *PHYB* (Figure 3). Segregating *LIGHT2* NIL progeny (Figure 5) were also genotyped at GPA1, a marker 14 cM distal to *PHYB*. Interval mapping using the *PHYB* and GPA1 markers and 100 CvL125 × L*er* F_2 plants showed that the likelihood and effect were greatest at *PHYB*, indicating that *LIGHT2* was closer to *PHYB* than GPA1. *phyB* loss-of-function mutations are recessive in these conditions; however, the less functional Cvi allele of *LIGHT2* is dominant (Figure 5). The Cvi allele of *LIGHT2* may therefore represent a dominant negative polymorphism in *PHYB*; however, ~200 other genes are in the 8-cM *LIGHT2* QTL interval.

DISCUSSION

We have identified 12 QTL that correspond to both candidate and unknown genes. Several QTL map to positions where no published candidate genes or photo-
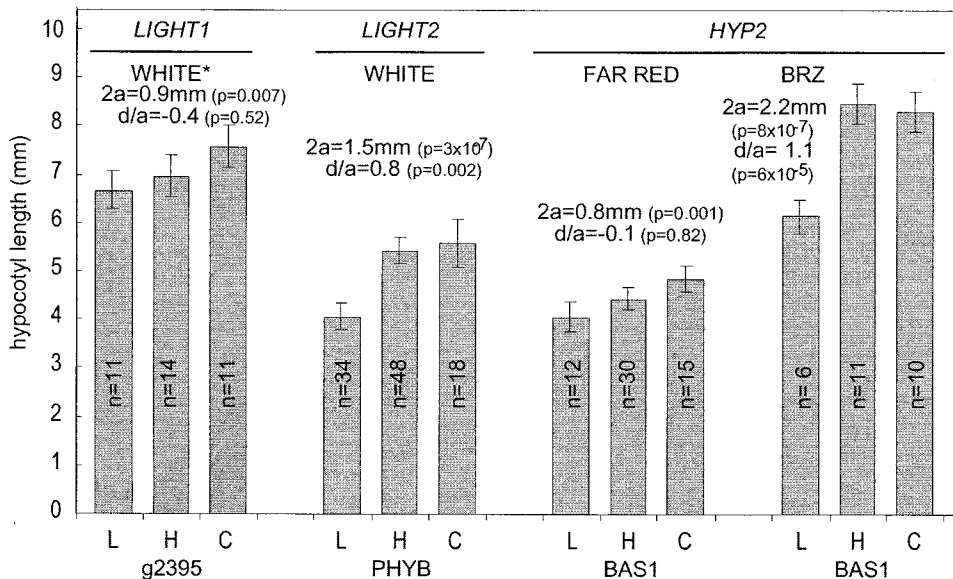

FIGURE 5.—Near isogenic lines. *LIGHT1*, *LIGHT2*, and *HYP2* NILs show the effect of a single QTL in segregating populations. Plants were grown in the indicated environment, measured, and genotyped at the marker g2395 for *LIGHT1*, *PHYB* for *LIGHT2*, or *BAS1* for *HYP2*; L, L*er*; H, heterozygote; C, Cvi. The QTL effect (2*a*) and dominance/additive ratio were estimated using linear regression. *n*, the number of seedlings genotyped in each class. Error bars represent 95% confidence intervals. The WHITE* environment has a reduced light fluence rate of 20 μE m^{-2} sec^{-1}.
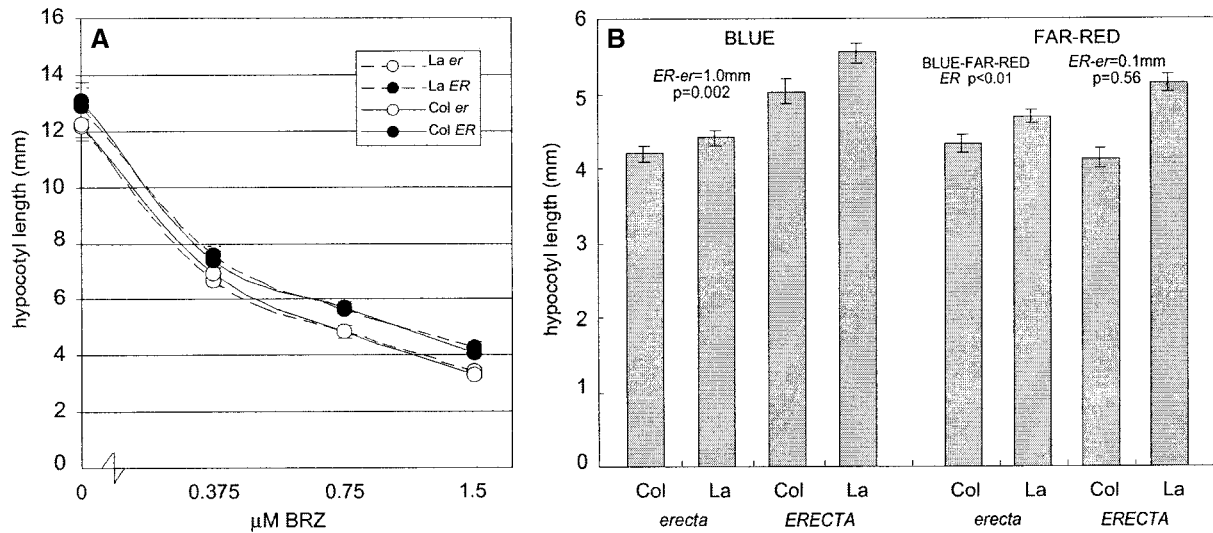
FIGURE 6.—*Erecta* effect. (A) BRZ dose response curve shows that *erecta* mutations in both the Col and La backgrounds reduce hypocotyl length equally across all inhibitor concentrations. The *x*-axis is on a log scale. (B) The *erecta* mutation causes a 1.0-mm decrease in hypocotyl length in blue light in both genetic backgrounds; however, no significant effect of *erecta* in far-red light was observed. The *erecta* effect is significantly different in blue and far-red light.

morphogenic mutations map, such as *HYP1*, *RED3*, *WHITE4*, *BLUE4*, *FARRED4*, and *BLUE5*. The major QTL *BRZ4* also describes a novel locus and has an effect that is large enough to make positional cloning a possibility. If the molecular nature of *BRZ4* can be identified it will uncover a new gene involved in brassinosteroid signaling and may help explain variation in hormone response among Arabidopsis accessions. In contrast, the confidence limits of the *DARK1* QTL overlap that of a Cvi/L*er* QTL affecting seed quality (ALONSO-BLANCO *et al.* 1999). Cvi alleles at this locus result in fewer seeds per fruit that are larger and heavier. Consequently more seed reserves may allow for an increased hypocotyl length in the dark. Cvi alleles also increase seed storability at this locus (BENTSINK *et al.* 2000). *DARK1* may be allelic to the QTL for seed quality traits. The *FARRED2* QTL maps to a region including the *SUPPRESSOR OF PHYA1* (*SPA1*) locus (HOECKER *et al.* 1998, 1999).

LIGHT1 represents a major locus responsible for light response variation between L*er* and Cvi across multiple light environments. Confidence limits of a major QTL affecting circadian rhythm, *ESPRESSO*, overlap with *LIGHT1* (SWARUP *et al.* 1999). This region also overlaps a minor QTL affecting flowering time (ALONSO-BLANCO *et al.* 1998a). The pleiotropic effects at the *LIGHT1* locus may be due to the action of more than one gene. However, several Arabidopsis mutants are known to affect hypocotyl length, circadian rhythm, and flowering time such as *LHY* and *CCA1* (SCHAFFER *et al.* 1998; WANG and TOBIN 1998), suggesting that there may be a single gene responsible for the effects in the *LIGHT1* region as well. The cloning of *LIGHT1* may identify a new and vital signaling component, as well as provide clues about the mechanisms of light response adaptation in natural populations.

Both the phenotype and map position of the *LIGHT2* QTL indicate *PHYB* as a candidate gene. We have sequenced *PHYB* from Cvi and L*er* and found considerable nucleotide variation in the promoter as well as synonymous and replacement changes in the coding region (J. N. MALOOF, J. LUTES, J. O. BOREVITZ, D. WEIGEL and J. CHORY, unpublished data). It is surprising that a photoreceptor may be a major light QTL, as loss-of-function *phyB* mutations have dramatic, deleterious effects throughout development. *phyB* null mutations also have a large effect on flowering time (REED *et al.* 1993). However, L*er*/Cvi flowering time QTL do not map to *PHYB* (ALONSO-BLANCO *et al.* 1998a). Thus, if *PHYB* is *LIGHT2*, this natural allele must affect only a subset of downstream processes controlled by PHYB. Further fine mapping of the *LIGHT2* QTL, as well as transgenic experiments with Cvi and L*er* alleles of *PHYB*, are needed to determine if *LIGHT2* is *PHYB*.

The *HYP2* locus exemplifies the difficulty in distinguishing between a single gene with effects in multiple environments and multiple genes in tight linkage with effects in specific environments. *HYP2* has effects in blue, far-red, BRZ, and dark and contributes to the high correlation between these environments (Table 3). The effect of *HYP2* in the blue and BRZ and dark environments is due to *erecta* (Figure 6, A and B). The far-red phenotype of *HYP2*, however, is likely not due to *erecta* (Figures 5 and 6B) and thus represents variation at another tightly linked gene. QTL analysis of the VLFR in the L*er*/Col RILs identified two QTL, *VLF1* and *VLF2* (YANOVSKY *et al.* 1997). *VLF1* affects cotyledon unfolding under short pulses of far-red light. The confidence limits of *VLF1* and *HYP2* overlap and they may be allelic. Differences in phenotypes between *VLF1* and *HYP2* may be due to differences between the Col and Cvi
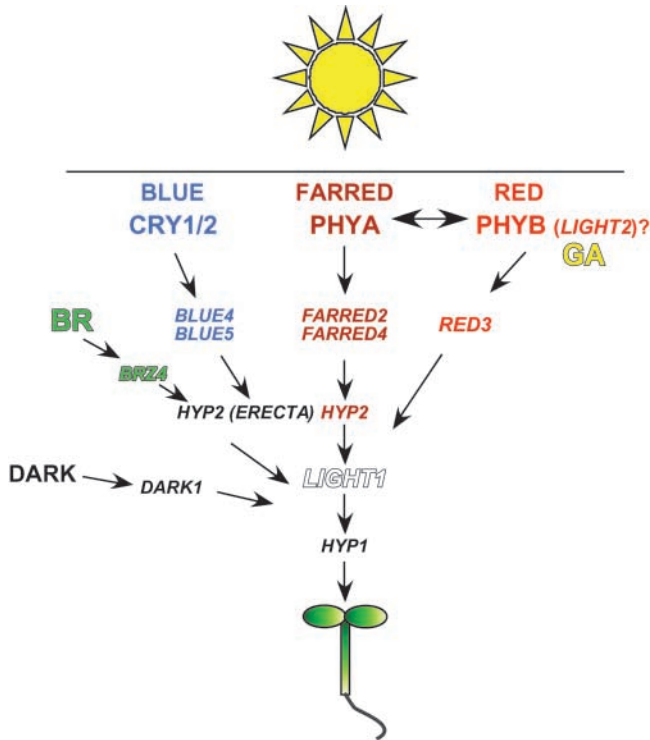
FIGURE 7.—QTL framework. A potential genetic pathway showing how light response QTL could act in different environments to control hypocotyl length. A strict gene order of action is not implied.

alleles at *VLF1/HYP2*, to other background effects, or to different genes responsible for *VLF1* and *HYP2* QTL.

Identifying epistatic interactions is a powerful advantage of QTL mapping over traditional approaches. The interacting loci on chromosome 5 together have an effect equal to that of the major light response QTL (Table 4), indicating that epistasis does account for some of the variation in hypocotyl length. Flowering time experiments have identified epistasis as an important factor in quantitative variation, with one interaction explaining up to 31% of the phenotypic variance (ALONSO-BLANCO *et al.* 1998a). The synergistic effect of *FRI* and *FLC* on late flowering, which is suppressible by vernalization, is also well established (LEE and AMASINO 1995). Approaches such as ours to detect epistasis may identify smaller but significant interactions that may be quite informative when candidate genes are considered. Others have also tested all markers for pairwise interactions and identified significant marker pairs that do not have large main effects on their own (SHOOK and JOHNSON 1999; SHIMOMURA *et al.* 2001).

In conclusion, we have mapped 12 highly significant hypocotyl length light and hormone response QTL from the L*er*/Cvi RIL population. Some QTL are unique to specific environments and have genotype-by-environment interactions, while others have effects in multiple environments. Figure 7 depicts a model in which QTL are placed into a genetic framework according to the environments in which they have phenotypes. Individ-

ual QTL can be crossed to other Arabidopsis photomorphogenic and hormone mutants and be integrated with the known signal transduction network (NEFF *et al.* 2000). *BLUE4* and *BLUE5* are specific to blue light and likely act downstream of the cryptochrome photoreceptors (Figure 7). The far-red light-specific effects of *HYP2*, *FARRED2*, and *FARRED4* suggest that they transduce signals from PHYA, the major photoreceptor in far-red light. The unique red light effect of *RED3* makes it a PHYB pathway candidate, since PHYB is the major photoreceptor in red light (Figure 7). The effect of *BRZ4* is specific to the BRZ environment and therefore may represent variation in brassinosteroid signaling or biosynthesis. The *DARK1* QTL affects hypocotyl length; however, its effect is overridden by light signals. The *HYP1* QTL may control length through a mechanism that is independent of light signals, possibly controlling cell size or cell number. *LIGHT1* may act downstream of multiple light and/or hormone signaling pathways and may serve to integrate multiple environmental cues. Finally *LIGHT2* may represent variation in a photoreceptor at the top of the light signaling hierarchy.

LITERATURE CITED

ALONSO-BLANCO, C., and M. KOORNNEEF, 2000   Naturally occurring variation in Arabidopsis: an underexploited resource for plant genetics. Trends Plant Sci. **5:** 22–29.

ALONSO-BLANCO, C., S. E.-D. EL-ASSAL, G. COUPLAND and M. KOORNNEEF, 1998a   Analysis of natural allelic variation at flowering time loci in the Landsberg erecta and Cape Verde Islands ecotypes of *Arabidopsis thaliana*. Genetics **149:** 749–764.

ALONSO-BLANCO, C., A. J. M. PEETERS, M. KOORNNEEF, C. LISTER, C. DEAN *et al.* 1998b   Development of an AFLP based linkage map of Ler, Col and Cvi *Arabidopsis thaliana* ecotypes and construction of a Ler/Cvi recombinant inbred line population. Plant J. **14:** 259–271.

ALONSO-BLANCO, C., H. BLANKESTIJN-DE VRIES, C. J. HANHART and M. KOORNNEEF, 1999   Natural allelic variation at seed size loci in relation to other life history traits of *Arabidopsis thaliana*. Proc. Natl. Acad. Sci. USA **96:** 4710–4717.

ARABIDOPSIS GENOME INITIATIVE, 2000   Analysis of the genome sequence of the flowering plant *Arabidopsis thaliana*. Nature **408:** 796–815.

ASAMI, T., and S. YOSHIDA, 1999   Brassinosteroid biosynthesis inhibitors. Trends Plant Sci. **4:** 348–353.

ASAMI, T., Y. K. MIN, N. NAGATA, K. YAMAGISHI, S. TAKATSUTO *et al.*,

2000 Characterization of brassinazole, a triazole-type brassino-steroid biosynthesis inhibitor. Plant Physiol. **123:** 93–99.

Bentsink, L., C. Alonso-Blanco, D. Vreugdenhil, K. Tesnier, S. P. Groot *et al.*, 2000 Genetic analysis of seed-soluble oligosaccharides in relation to seed storability of Arabidopsis. Plant Physiol. **124:** 1595–1604.

Casal, J. J., and H. Smith, 1989 The function action and adaptive significance of phytochrome in light-grown plants. Plant Cell Environ. **12:** 855–862.

Chory, J., and J. Li, 1997 Gibberellins, brassinosteroids and light-regulated development. Plant Cell Environ. **20:** 801–806.

Doerge, R. W., and G. A. Churchill, 1996 Permutation tests for multiple loci affecting a quantitative character. Genetics **142:** 285–294.

Efron, B., and R. Tibshirani, 1993 *An Introduction to the Bootstrap.* Chapman & Hall, New York.

Haley, C. S., and S. A. Knott, 1992 A simple regression method for mapping quantitative trait loci in line crosses using flanking markers. Heredity **69:** 315–324.

Hoecker, U., Y. Xu and P. H. Quail, 1998 *SPA1*: a new genetic locus involved in phytochrome A-specific signal transduction. Plant Cell **10:** 19–33.

Hoecker, U., J. M. Tepperman and P. H. Quail, 1999 SPA1, a WD-repeat protein specific to phytochrome A signal transduction. Science **284:** 496–499.

Houle, D., 1992 Comparing evolvability and variability of quantitative traits. Genetics **130:** 195–204.

Hsieh, H. L., H. Okamoto, M. Wang, L. H. Ang, M. Matsui *et al.*, 2000 *FIN219*, an auxin-regulated gene, defines a link between phytochrome A and the downstream regulator COP1 in light control of Arabidopsis development. Genes Dev. **14:** 1958–1970.

Ihaka, R., and R. Gentleman, 1996 R: a language for data analysis and graphics. J. Comput. Graph. Stat. **5:** 299–314.

Jansen, R. C., 1993 Interval mapping of multiple quantitative trait loci. Genetics **135:** 205–211.

Jansen, R. C., and P. Stam, 1994 High resolution of quantitative traits into multiple loci via interval mapping. Genetics **136:** 1447–1455.

Jiang, C., and Z-B. Zeng, 1995 Multiple trait analysis of genetic mapping for quantitative trait loci. Genetics **140:** 1111–1127.

Juenger, T., M. Purugganan and T. F. Mackay, 2000 Quantitative trait loci for floral morphology in *Arabidopsis thaliana*. Genetics **156:** 1379–1392.

Kao, C.-H., 2000 On the differences between maximum likelihood and regression interval mapping in the analysis of quantitative trait loci. Genetics **156:** 855–865.

Kendrick, R. E., and G. H. M. Kronenberg, 1994 *Photomorphogenesis in Plants.* Kluwer Academic, Dordrecht The Netherlands/Boston.

Knapp, S. J., W. C. Bridges, Jr. and D. Birkes, 1990 Mapping quantitative trait loci using molecular marker linkage maps. Theor. Appl. Genet. **79:** 583–592.

Konieczny, A., and F. M. Ausubel, 1993 A procedure for mapping Arabidopsis mutations using co-dominant ecotype-specific PCR-based markers. Plant J. **4:** 403–410.

Krysan, P. J., J. C. Young and M. R. Sussman, 1999 T-DNA as an insertional mutagen in Arabidopsis. Plant Cell **11:** 2283–2290.

Lee, I., and R. M. Amasino, 1995 Effect of vernalization, photoperiod, and light quality on the flowering phenotype of Arabidopsis plants containing the *FRIGIDA* gene. Plant Physiol. **108:** 157–162.

Li, J., and J. Chory, 1997 A putative leucine-rich repeat receptor kinase involved in brassinosteroid signal transduction. Cell **90:** 929–938.

Li, J., P. Nagpal, V. Vitart, T. C. McMorris and J. Chory, 1996 A role for brassinosteroids in light-dependent development of Arabidopsis. Science **272:** 398–401.

Maloof, J. N., J. O. Borevitz, D. Weigel and J. Chory, 2000 Natural variation in phytochrome signaling. Semin. Cell Dev. Biol. **11:** 523–530.

Maloof, J. N., J. O. Borevitz, T. Dabi, J. Lutes, R. B. Nehring *et al.*, 2001 Natural variation in light sensitivity of Arabidopsis. Nat. Genet. **29:** 441–446.

Neff, M. M., S. M. Nguyen, E. J. Malancharuvil, S. Fujioka, T. Noguchi *et al.*, 1999 *BAS1*: a gene regulating brassinosteroid

levels and light responsiveness in Arabidopsis. Proc. Natl. Acad. Sci. USA **96:** 15316–15323.

Neff, M. M., C. Fankhauser and J. Chory, 2000 Light: an indicator of time and place. Genes Dev. **14:** 257–271.

Nettleton, D., and R. W. Doerge, 2000 Accounting for variability in the use of permutation testing to detect quantitative trait loci. Biometrics **56:** 52–58.

Parinov, S., M. Sevugan, Y. De, W. C. Yang, M. Kumaran *et al.*, 1999 Analysis of flanking sequences from *Dissociation* insertion lines: a database for reverse genetics in Arabidopsis. Plant Cell **11:** 2263–2270.

Pinheiro, J. C., and D. M. Bates, 2000 *Mixed-Effects Models in S and S-Plus.* Springer-Verlag, New York.

Reed, J. W., P. Nagpal, D. S. Poole, M. Furuya and J. Chory, 1993 Mutations in the gene for the red/far-red light receptor *phytochrome B* alter cell elongation and physiological responses throughout Arabidopsis development. Plant Cell **5:** 147–157.

Reed, J. W., K. R. Foster, P. W. Morgan and J. Chory, 1996 *Phytochrome B* affects responsiveness to gibberellins in Arabidopsis. Plant Physiol. **112:** 337–342.

Robertson, A., 1959 The sampling variance of the genetic correlation coefficient. Biometrics **15:** 469–485.

Schaffer, R., N. Ramsay, A. Samach, S. Corden, J. Putterill *et al.*, 1998 The *late elongated hypocotyl* mutation of Arabidopsis disrupts circadian rhythms and the photoperiodic control of flowering. Cell **93:** 1219–1229.

Scheffé, H., 1959 *The Analysis of Variance.* John Wiley & Sons, New York.

Schmitt, J., S. A. Dudley and M. Pigliucci, 1999 Manipulative approaches to testing adaptive plasticity: phytochrome-mediated shade-avoidance responses in plants. Am. Nat. **154:** S43–S54.

Shimomura, K., S. S. Low-Zeddies, D. P. King, T. D. Steeves, A. Whiteley *et al.*, 2001 Genome-wide epistatic interaction analysis reveals complex genetic determinants of circadian behavior in mice. Genome Res. **11:** 959–980.

Shook, D. R., and T. E. Johnson, 1999 Quantitative trait loci affecting survival and fertility-related traits in *Caenorhabditis elegans* show genotype-environment interactions, pleiotropy and epistasis. Genetics **153:** 1233–1243.

Smith, H., 1995 Physiological and ecological function within the phytochrome family. Annu. Rev. Plant Physiol. Plant Mol. Biol. **46:** 289–315.

Swarup, K., C. Alonso-Blanco, J. R. Lynn, S. D. Michaels, R. M. Amasino *et al.*, 1999 Natural allelic variation identifies new genes in the Arabidopsis circadian system. Plant J. **20:** 67–77.

Tian, Q., and J. W. Reed, 1999 Control of auxin-regulated root development by the *Arabidopsis thaliana SHY2/IAA3* gene. Development **126:** 711–721.

Torii, K. U., N. Mitsukawa, T. Oosumi, Y. Matsuura, R. Yokoyama *et al.*, 1996 The Arabidopsis *ERECTA* gene encodes a putative receptor protein kinase with extracellular leucine-rich repeats. Plant Cell **8:** 735–746.

Vos, P., R. Hogers, M. Bleeker, M. Reijans, T. van de Lee *et al.*, 1995 AFLP: a new technique for DNA fingerprinting. Nucleic Acids Res. **23:** 4407–4414.

Wang, Z. Y., and E. M. Tobin, 1998 Constitutive expression of the *CIRCADIAN CLOCK ASSOCIATED 1* (*CCA1*) gene disrupts circadian rhythms and suppresses its own expression. Cell **93:** 1207–1217.

Yamamuro, C., Y. Ihara, X. Wu, T. Noguchi, S. Fujioka *et al.*, 2000 Loss of function of a *Rice brassinosteroid insensitive1* homolog prevents internode elongation and bending of the lamina joint. Plant Cell **12:** 1591–1606.

Yanovsky, M. J., J. J. Casal and J. P. Luppi, 1997 The *VLF* loci, polymorphic between ecotypes Landsberg erecta and Columbia, dissect two branches of phytochrome A signal transduction that correspond to very-low-fluence and high-irradiance responses. Plant J. **12:** 659–667.

Zeng, Z-B., 1994 Precision mapping of quantitative trait loci. Genetics **136:** 1457–1468.

Zhao, Y., S. K. Christensen, C. Fankhauser, J. R. Cashman, J. D. Cohen *et al.*, 2001 A role for flavin-containing monooxygenases in auxin biosynthesis. Science **291:** 306–309.

Communicating editor: T. F. C. Mackay